Separation Science and Technology
Publication details, including instructions for authors and subscription information:
http://www.informaworld.com/smpp/title~content=t713708471

Quantitative Analysis and Equilibrium Models of Selective Adsorption in Multimetal Systems Using a Bacterial Biosorbent

Jo-Shu Chang; Chia-Chi Chen

To cite this Article Chang, Jo-Shu and Chen, Chia-Chi(1998) 'Quantitative Analysis and Equilibrium Models of Selective Adsorption in Multimetal Systems Using a Bacterial Biosorbent', Separation Science and Technology, 33: 5, 611 — 632
To link to this Article: DOI: 10.1080/01496399808544779
URL: http://dx.doi.org/10.1080/01496399808544779

SEPARATION SCIENCE AND TECHNOLOGY, 33(5), pp. 611–632, 1998

Quantitative Analysis and Equilibrium Models of Selective Adsorption in Multimetal Systems Using a Bacterial Biosorbent

JO-SHU CHANG* and CHIA-CHI CHEN
DEPARTMENT OF CHEMICAL ENGINEERING
FENG CHIA UNIVERSITY
TAICHUNG, TAIWAN, REPUBLIC OF CHINA
TELEPHONE: 886-4-4517250 EXT. 3651
FAX: 886-4-4510890

ABSTRACT

This study investigated the behavior of selective adsorption on the biomass of *Pseudomonas aeruginosa* PU21 (Rip64) with solutions containing Pb, Cu, and Cd. Experiments were designed to quantitatively justify the biosorption preference of the biomass for the three metals. The multimetal adsorption equilibria were described by three models, two of which originated from single-component Langmuir isotherm, and the third one was established empirically. The multimetal adsorption results show that lead and copper significantly inhibited the adsorption of cadmium, while the effects of Cd on the adsorption of Cu and Pb were limited. Lead was found to exhibit a slightly higher inhibition effect on Cu when the two adsorbate coexisted. The data obtained from the ion-exchange systems indicate that Pb and Cu appreciably replaced the preadsorbed Cd ions from the biosorbent, but the competition of Pb and Cu for the adsorption sites was comparative. For three-metal biosorption with equal initial molar concentrations, the relative surface coverage of Pb, Cu, and Cd on the biomass was approximately 55, 40, and 5%, respectively. A modified Langmuir-type model (Model 2), which took account of the heterogeneity and specificity of the adsorption sites, described the experimental results better than the traditional Langmuir isotherm (Model 1) did. Of the three models examined, the empirical one (Model 3) showed the best fits for the two-metal adsorption data, whereas Model 2 had better prediction for the ternary adsorption results. In Model 3 the parameters determined from binary systems can be extrapolated to predict the adsorption equilibria of three-metal adsorption systems satisfactorily.

* To whom correspondence should be addressed.

INTRODUCTION

Since Ruchloft (1) found that uranium ions in radioactive wastes can be immobilized by microorganisms in an activated sludge process, adsorption or accumulation of heavy metals by a biomass of algae, fungi, and bacteria has received much attention recently due to its potential use in waste treatment processes involving removal of heavy-metal pollutants from a contaminated environment (2). The research on so-called biosorption or bioaccumulation has been performed with a variety of aspects as summarized in a recent review by Volesky and Holan (3). The research on biosorption of heavy metals in the past mainly investigated either the adsorption efficiencies and equilibria for different biosorbent materials (4) or the development of batch or continuous biosorption processes (5–7). However, relatively less work has been contributed to elucidate the details of the biosorption behavior in multimetal systems, which are normally the composition of the industrial effluents (7). For more effective applications of metal biosorbents, more in-depth investigations are still required to identify the selectivity of biosorbents for the coexisting metal ions, so that the efficiency of the biosorption process can be estimated prior to the treatment and the operation strategies can thereby be optimized.

Our previous report (8) showed that inactivated cells of *Pseudomonas aeruginosa* PU21 (Rip64) was able to selectively adsorb Hg^{2+} over Na^{+} with maximal capacity of nearly 400 mg Hg/g dry cell. Resting cells of the strain were also capable of adsorbing lead, copper, and cadmium effectively (9). In this research we utilized the biosorbent to quantitatively reveal the co-ion effects on the selective biosorption and to build up mathematical models for the description and prediction of adsorption equilibria of multicomponent systems. The metals of interest were lead, copper, and cadmium, which are commonly found in the industrial effluents in Taiwan. For a systematic evaluation of selective adsorption, two kinds of adsorption systems were conducted; one was *co-ion systems* in which two or three metals coexisted, and the other was *ion-exchange systems* in which the biomass was saturated with one metal prior to exposure to the second metal. This research aimed to present a methodology for the analysis of selective adsorption data to provide a clearer picture of how coadsorbates compete for the adsorption sites, and to predict multicomponent adsorption equilibria quantitatively based upon the initial metal compositions in the solutions. This effort is expected to benefit and supplement further development of practical biosorption processes for heavy-metal removal.

EXPERIMENTAL METHODS

Bacterial Strain and Cultivation

Pseudomonas aeruginosa PU21, an auxotrophic derivative of PAO1, was isolated from clinical sewage by Jacoby (10). The strain harbors a 142.5 Kb

plasmid Rip64 which encodes for the narrow-spectrum mercury resistance in addition to resistance to various antibiotics (10). The strain was cultivated in Luria-Bertani (LB) broth (Difco), which was amended with 25–50 mg Hg^{2+}/L to avoid contamination from other microorganisms. The bacterial cultures were incubated aerobically at 37°C, and the liquid cultures were constantly agitated at 220 rpm in glass flasks.

Preparation of Biosorbents

Cells of *P. aeruginosa* PU21 were harvested by centrifugation (15,000 *g*, 8 minutes) from early-stationary cultures with a cell density of approximately 1–2 g/L. After being rinsed twice with deionized, reverse osmotically treated (RO) water, the cells were resuspended in designated heavy metal solutions also prepared with deionized RO water for the biosorption experiments. All the glassware used in the biosorption operations was treated with concentrated HNO_3 solution prior to each experiment to avoid possible adsorption of heavy metals on the glass surface.

Measurement of Heavy Metals

The heavy metal adsorbates used in this study were $Pb(NO_3)_2$, $CuCl_2{\cdot}2H_2O$, and $CdCl_2$, which were obtained from Riedel-de Haen, Inc. Heavy metal contents in solutions were measured with a Polarized Zeeman Atomic Absorption Spectrometer (Hitachi Model-Z-6100).

Procedures of Selective Biosorption Experiments

Adsorption Isotherms

Biomass of *P. aeruginosa* PU21 (1–2 g/L) were suspended in solutions amended with one of the three metal ions (Pb^{2+}, Cu^{2+}, Cd^{2+}) in the 0–2000 μM concentration range. The cell suspensions were also added into binary and ternary mixtures of the three metals to determine adsorption isotherms for the multimetal systems. In all cases the adsorption solutions were gently agitated at 37°C, and pH values of the solutions were adjusted to 5.0 initially. The pH value of 5.0 was chosen to prevent possible metal precipitation as hydroxides. As the adsorption reached equilibrium, samples were taken from the solution, and centrifuged to separate the biomass and metal solutions, and the metal concentrations in the supernatant were measured.

Co-Ion Systems

The biosorbent with a concentration of 1–2 g cell/L was suspended in binary or ternary mixtures of Pb^{2+}, Cu^{2+}, and Cd^{2+} in the 0–2000 μM concen-

tration range. The adsorption solutions were gently agitated at 37°C, and the initial pH was adjusted to 5.0. Samples were taken from the solution at desired time intervals, and the heavy metal concentration in the supernatant was determined.

Ion-Exchange Systems

The biosorbent (1–2 g cell/L) was mixed with one of the three metal ions until saturation was reached. The metal-laden biosorbent was harvested and resuspended in solutions containing the second metal ions in the 0–3000 μM concentration range. The biosorption was carried out at pH 5.0 and 37°C. Procedures of sampling and metal measurement were identical to those described for co-ion systems.

RESULTS AND DISCUSSION

Biosorption Isotherms in Single and Multimetal Systems

Figures 1 to 4 demonstrate the adsorption isotherms of Pb, Cu, and Cd in single-metal, two-metal, and three-metal systems. The symbols in the figures represent the experimental data, while the curves were generated by Langmuir isotherm for single-component adsorption, and by three proposed models (which will be discussed later) for multicomponent adsorption. Figures 1–3 demonstrate how the two coadsorbates affected each other on their adsorption equilibria as compared with results from single-component adsorption. It was clearly observed that adsorption of Cd was significantly inhibited by coexisting Pb and Cu (Figs. 2b and 3b), whereas the presence of Cd did not appreciably affect the adsorption of Cu and Pb (Figs. 2a and 3a). However, the competition between Cu and Pb ions for the adsorption sites was relatively comparative (Figs. 1a and 1b). Figure 4 illustrates adsorption isotherms of Pb^{2+}, Cu^{2+}, and Cd^{2+} obtained from three-component adsorption. It shows that when the three metals coexisted, the saturation capacities of all three metals dropped significantly (Figs. 1–4, Table 1). It is worth noting that the biomass had the highest saturation capacity for copper in the single-metal system, followed by lead and cadmium (Table 1), whereas in three-metal adsorption the maximal capacity of the metals decreased in the order of Pb > Cu > Cd (Table 1). This observation seems to suggest that the biomass inherently had the highest total capacity for copper, but in co-ions adsorption lead was most favorable. More detailed comments on the capacity and preference of the biomass for the three metals of interest will be discussed in succeeding sections.

Table 1 summarizes the maximal total and individual metal capacities of the biomass for biosorption carried out with single and multiple adsorbates.

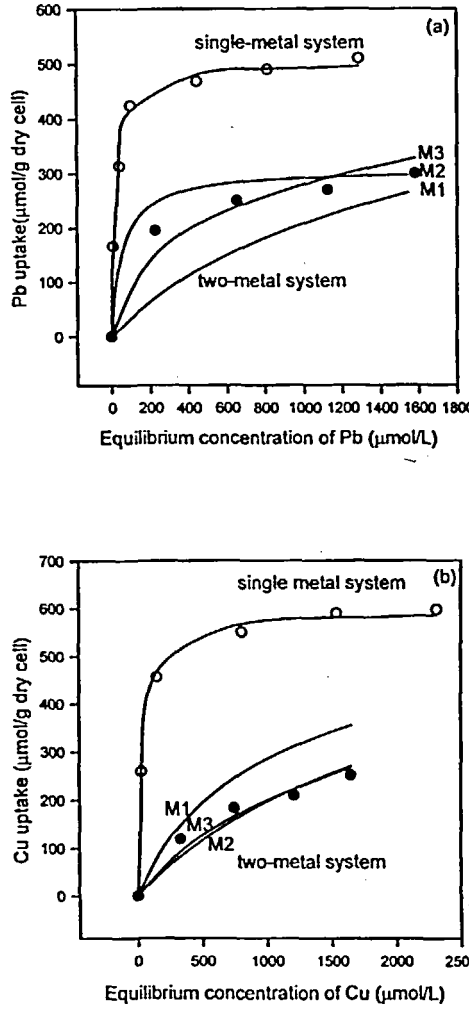

FIG. 1 Comparison of adsorption isotherms between single-metal and two-metal systems by *Pseudomonas aertuginosa* PU21 (biomass concentration: 1.45 g/L). (a) The isotherm of Pb with and without the presence of 2000 μM Cu; (b) the isotherm of Cu with and without the presence of 2000 μM Pb. (Open symbols: experimental data from single metal adsorption. Closed symbols: experimental data from binary adsorption. Dashed lines: simulation by Langmuir model. Solid lines: simulation by the proposed models. M1: Model 1; M2: Model 2; M3: Model 3.)

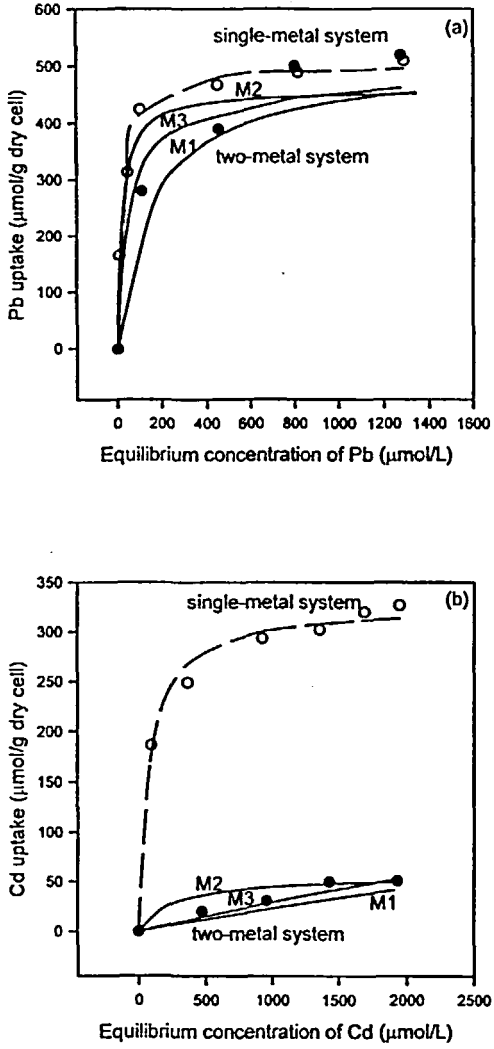

FIG. 2 Comparison of adsorption isotherms between single-metal and binary systems by *Pseudomonas aeruginosa* PU21 (biomass concentration: 1.45 g/L). (a) The isotherm of Pb with and without the presence of 2000 μM Cd; (b) the isotherm of Cd with and without the presence of 2000 μM Pb. (Open symbols: experimental data from single metal adsorption. Closed symbols: experimental data from binary adsorption. Dashed lines: simulation by Langmuir model. Solid lines: simulation by the proposed models. M1: Model 1; M2: Model 2; M3: Model 3.)

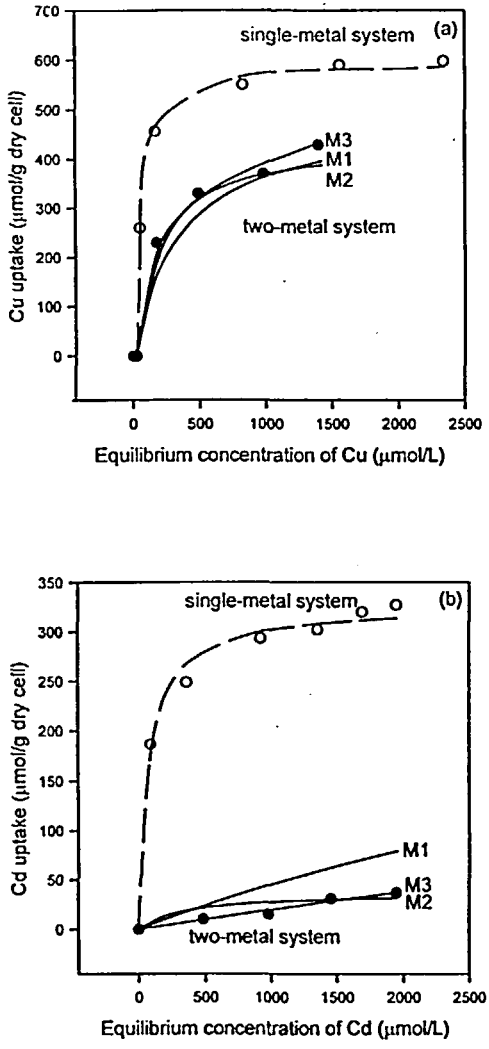

FIG. 3 Comparison of adsorption isotherms between single-metal and binary systems by *Pseudomonas aeruginosa* PU21 (biomass concentration: 1.45 g/L). (a) The isotherm of Cu with and without the presence of 2000 μM Cd; (b) the isotherm of Cd with and without the presence of 2000 μM Cu. (Open symbols: experimental data from single metal adsorption. Closed symbols: experimental data from binary adsorption. Dashed lines: simulation by Langmuir model. Solid lines: simulation by the proposed models. M1: Model 1; M2: Model 2; M3: Model 3.)

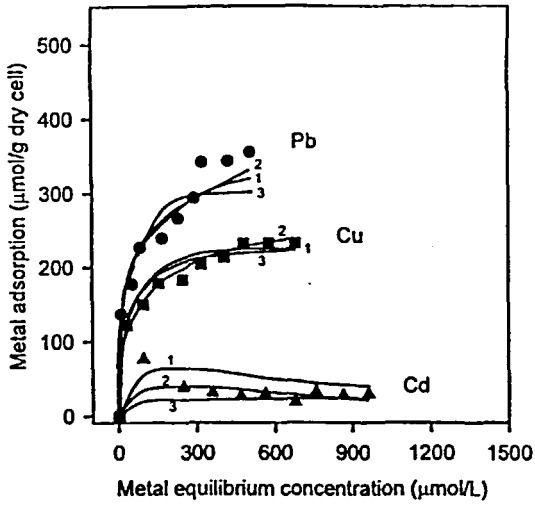

FIG. 4 Isotherms from three-metal adsorption of Pb, Cu, and Cd by *Pseudomonas aeruginosa* PU21 (biomass concentration: 1.80 g/L). (Symbols: experimental data. Solid lines: simulation by the proposed models. M1: Model 1; M2: Model 2; M3: Model 3.)

It indicates that the maximal total capacity resulting from single, binary, and ternary systems was 600 μmol/g (for Cu alone), 642 μmol/g (for Cu + Pb), and 615 μmol/g (for Cu + Pb + Cd), respectively. As the saturation capacity for Cu alone was essentially equivalent to the maximal capacities obtained

TABLE 1
Maximal Individual and Overall Capacities of the Biomass for Pb, Cu, and Cd in Single, Binary, and Ternary Systems

	Adsorption systems											
	Single-component adsorption			Two-component adsorption						Three-component adsorption		
				Pb–Cu		Pb–Cd		Cu–Cd				
Adsorbates	Pb	Cu	Cd	Pb	Cu	Pb	Cd	Cu	Cd	Pb	Cu	Cd
Capacity for each component (μmol/g dry cell)	520	600	327	337	305	508	65	563	42	345	231	39
Overall capacity (μmol/g dry cell)		—		642		573		605			615	

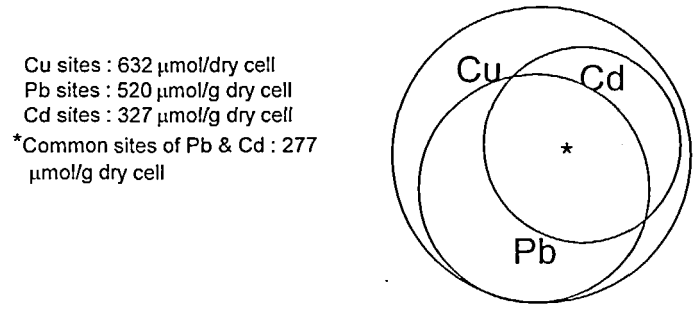

FIG. 5 Schematic description of proposed relative surface coverage distribution of Pb, Cu, and Cd on the biomass of *Pseudomonas aeruginosa* PU21.

from two-metal and three-metal systems, it seems reasonable to assume that the total number of copper adsorption sites on the biosorbent represented roughly the total number of adsorption sites for the three metals together. On the other hand, since the maximal capacity for the Pb + Cd system was larger than that for a single system of Pb or Cd, the adsorption sites of Pb and Cd were likely to be partially overlapped. Based upon the arguments stated above, the distribution of surface adsorption sites of Cu, Pb, and Cd on the biomass can be proposed as described schematically in Fig. 5. The information provided in Fig. 5 apparently violates basic assumptions of the Langmuir models (11) which propose that the entire adsorbent surface is homogeneous and that there is no lateral interaction between adsorbate molecules, and thus the affinity of each binding site for the adsorbate molecules should be uniform. As a result, the adsorbent should have identical maximum capacity for each adsorbate present. Therefore, Langmuir models simply cannot account for the adsorption equilibrium when the adsorbent appears to have specific binding sites and a distinct preference for each adsorbate.

Selective Adsorption of Lead, Copper, and Cadmium in Co-Ion Systems

The selectivity of biomass of *P. aeruginosa* PU21 for Pb, Cu, and Cd was evaluated with binary or ternary mixtures of the three metals. In binary systems, one metal (metal A) at an initial concentration of 2000 μM was mixed with elevated concentrations (from 0 to 2000 μM) of the other metal ions (metal B) in order to observe the effects of metal B on the adsorption of metal A. Adsorption preference was also observed in ternary systems consisting of equal molar concentrations of each metal component. The results are described and discussed as follows.

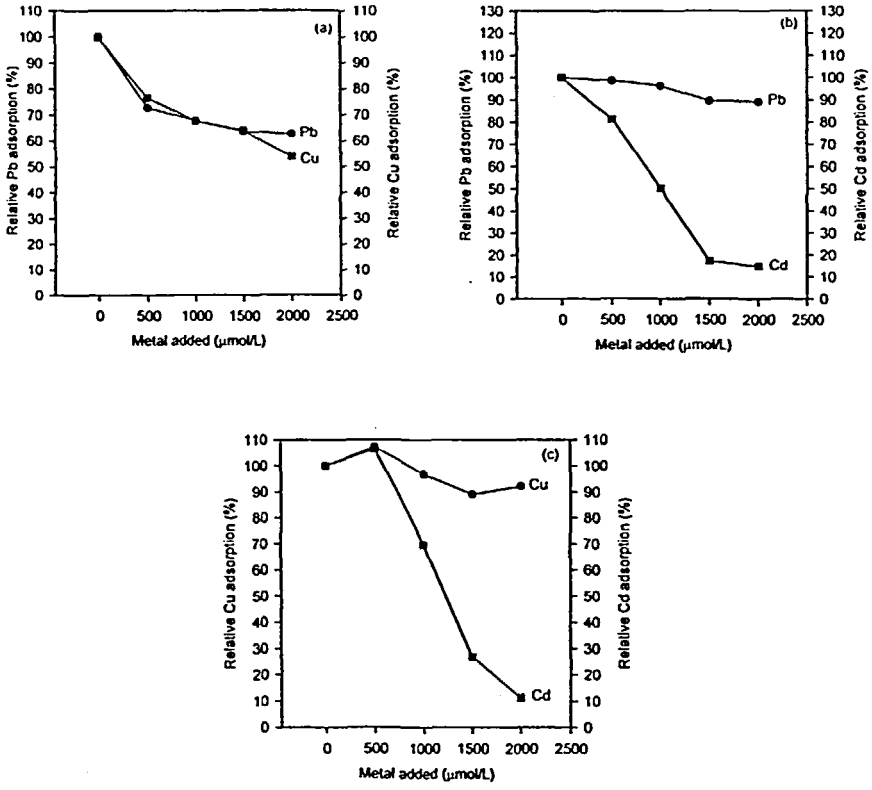

FIG. 6 Effect of metal B on the adsorption of metal A by *Pseudomonas aeruginosa* PU21 (biomass concentration: 1.45 g/L) from binary mixtures of Pb, Cu, and Cd. Initial concentration of metal A was fixed at 2000 μM, and metal B concentration was increased from 0 to 2000 μM. Metal A/B = (a) ●: Pb/Cu, ■: Cu/Pb; (b) ●: Pb/Cd, ■: Cd/Pb; (c) ●: Cu/Cd, ■: Cd/Cu.

$$\text{Relative metal A adsorption} = \frac{\text{metal A adsorption capacity with the coexistence of metal B}}{\text{metal A adsorption capacity without the coexistence of metal B}} \times 100\%$$

Binary Systems

Figure 6(a) demonstrates the competition of biosorption for Pb and Cu on the biosorbent. With the initial Pb concentration fixed at 2000 μM, the adsorption capacity of Pb decreased as Cu concentrations were increased from 0 to 2000 μM (Fig. 6a). When initial concentrations of Pb and Cu were both at 2000 μM, the adsorption of Pb decreased to 37% of its original capacity.

In the reverse operation, addition of Pb also reduced the capacity of Cu adsorption with a similar trend (Fig. 6a), but Cu decreased to 46% of its original capacity as the concentrations of Cu and Pb were both equal to 2000 μM. As shown in Fig. 6(b), as 0–2000 μM of Cd was added into solutions originally containing 2000 μM of lead, the Pb adsorption maintained over 90% of its single-component adsorption capacity. However, with a fixed Cd concentration and increased Pb concentrations, the adsorption of Cd was significantly decreased, and the biomass could barely adsorb Cd when both Pb and Cd had the same initial concentration of 2000 μM (Fig. 6b). The competition of Cu and Cd over the biosorbent is illustrated in Fig. 6(c). Similar to the results observed for the Pb/Cd system, the Cu ions exhibited tremendous inhibition effects on the biosorption of Cd, while Cu adsorption remained above 90% of its original capacity despite the addition of a high concentration (2000 μM) of Cd (Fig. 6c). The results shown in Fig. 6 clearly indicate that the biomass had a higher preference for Pb over Cu, and biosorption of Cd was overwhelmed by the competition of Pb and Cu.

Ternary Systems

Figures 7(a) and 7(b) demonstrate the behavior of the selective adsorption of Pb, Cu, and Cd when the biomass was exposed to equal molar concentrations of the three metals. The experimental data are presented in terms of the adsorption efficiency ($Q_M\%$), and the relative coverage ($\theta_M\%$), whose definitions are as follows:

$$Q_M\% = \frac{\text{moles of metal M adsorbed}}{\text{moles of metal M added}} \times 100\%$$

and

$$\theta_M\% = \frac{\text{moles of metal M adsorbed}}{\text{moles of all three metals adsorbed}} \times 100\%$$

The values of $Q_M\%$ and $\theta_M\%$ are indications of the relative adsorption preference and distribution of each metal of interest on the biosorbent. According to the results shown in Fig. 7(a), an increase in the initial metal concentration led to a decrease in the adsorption efficiency ($Q_M\%$) of each metal. For all initial concentrations detected, the adsorption efficiency of the three metals was in the order $Q_{Pb}\% > Q_{Cu}\% > Q_{Cd}\%$. It was also observed that the decrease of $Q_{Cd}\%$ responding to the increase of initial concentration was most significant. As the initial concentration of each metal was over 400 μM, the $Q_{Cd}\%$ value dropped to below 10%, whereas the decline of $Q_{Pb}\%$ and $Q_{Cu}\%$ was less steep (Fig. 7a). The rate and extent of the decrease in $Q_M\%$ shown in Fig. 7(a) imply that the adsorption preference of the biosorbent was

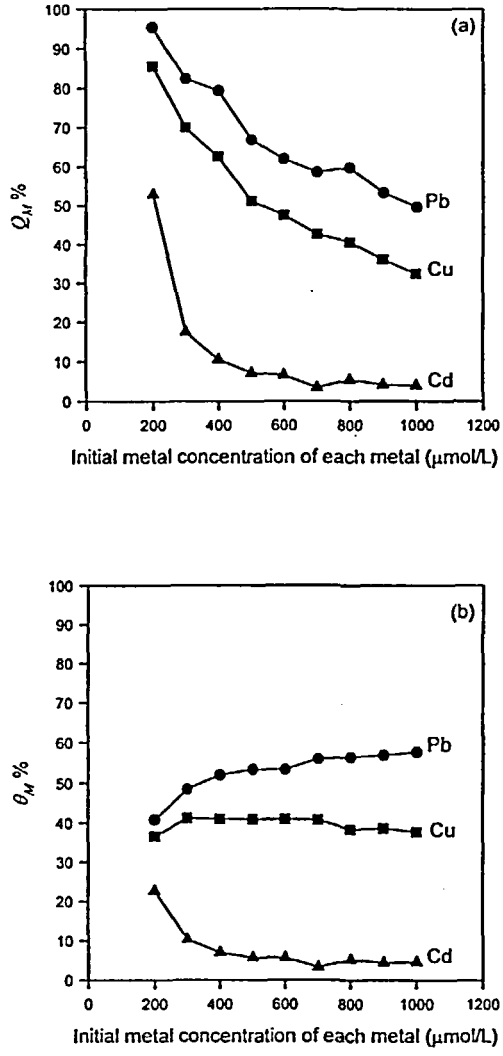

FIG. 7 Selective biosorption in ternary mixtures containing equal molar concentrations of Pb, Cu, and Cd by *Pseudomonas aeruginosa* PU21 (biomass concentration: 1.80 g/L). (a) Dependence of adsorption efficiency (Q_M%) of Pb, Cu, and Cd on initial concentrations of each metal; (b) dependence of relative coverage (θ_M%) on initial concentrations of each metal.

TABLE 2
Correlation of Properties of Metals and Biosorbents with Metal Adsorption Preference

	Hg	Pb	Cu	Ni	Cd	Zn	Biosorbent	Reference
Standard reduction potentials (V)	0.851	−0.1263	0.3402	−0.23	−0.4026	−0.7628		Bodner and Pardue (16)
Electronegativity	2.00	2.33	1.90	1.91	1.69	1.65		
Ionic radii (nm)	0.110	0.120	0.072	0.069	0.097	0.074		
Atomic weight	200.59	207.2	63.546	58.69	112.41	65.38		
Order of adsorption preference	1	2	3	4	5	6	*Pseudomonas saccharophilia*	Nakajima and Sakaguchi (12)
	1	2	3	5	4	6	*Bacillus subtilis*	
	—	—	1	—	2	3	*Ascophyllum nodosum*	DeCarvalho et al. (13)
	—	1	2	5	4	3	*Streptomycetes noursei*	Mattuschka and Straube (14)[a]
	—	—	1	—	2	3	*Penicillum chrysogemum*	Pighi et al. (15)
	—	1	2	—	3	—	*Pseudomonas aeruginosa*	This study

[a] Single-component adsorption

Pb > Cu > Cd. The trend that Q_M% decreased with the increase of initial metal concentration seems reasonable since the relative number of binding sites available to each metal would reduce as the concentrations of the three metals were increased simultaneously, especially when the biomass was nearly saturated at high initial concentrations.

The selective adsorption in the ternary system was also evaluated in terms of relative coverage (θ_M%) of each metal as demonstrated in Fig. 7(b). It shows that Pb owned the highest relative coverage (θ_{Pb}%) of 40–55% over the range of the initial concentrations used. The relative coverage of Cu (θ_{Cu}%) was slightly lower with a value of 35–40%, while the value of θ_{Cd}% was the lowest among the three metals, and dropped to below 10% when the initial concentration of each metal was greater than 400 μM. In contrast to significant deviations of Q_M% over the metal concentration range used, the relative coverage of the three metals did not vary considerably at all concentrations detected (Fig. 7b), especially when the initial concentration was above 400 μM. In this range θ_{Pb}%, θ_{Cu}%, and θ_{Cd}% exhibited a nearly constant ratio of 55:40:5. Therefore, the relative coverage data make it more apparent that the dominance of selective biosorption was in the order Pb > Cu > Cd.

Factors that affect the adsorption preference of a biosorbent for metal adsorbates may be related to the characteristics of the binding sites (e.g., functional groups, structure, etc.) and the properties of the metal adsorbates (e.g., ionic size, atomic weight, or reduction potential of the metal). Table 2 summarizes

the correlation between the chemical and physical properties of the metal and the selective adsorption of the metals by a variety of biosorbents. It appears complicated to find a common rule from Table 2 to identify how metal properties affect the selective adsorption. This is because the observed behavior may result from a combination of all the above factors. Nevertheless, there is a general trend, which is that an increase in the reduction potential, electronegativity, and atomic weight leads to a higher adsorption preference by the biosorbent. The effects of ionic radius are, however, relatively unclear. This trend seems acceptable because metals with a higher reduction potential or electronegativity tend to exhibit a stronger ionic interaction with an electron-rich surface of biosorbents. The movement of metals with a higher atomic weight can generate higher momentum energy, which may facilitate the adsorption of the metal by increasing the probability of effective collision between the metal and the surface. It is evident from Table 2 that the order of metal adsorption preference does not necessarily follow the general trends described above. This inconsistency most likely originates from variations in composition and structure of the biosorbent surface, since the trend was deduced primarily on the basis of the properties of metals without consideration for the effects of the characteristics of biosorbent materials. As indicated in Table 2, our finding on the order of adsorption preference of Pb, Cu, and Cd is essentially consistent with those observed on different biosorbent materials with only one exception (12–14). However, none of the previous investigations provided quantitative details of selective adsorption, such as the extent of selectivity or the relative surface coverage of each coadsorbate during selective biosorption. This information can be obtained from this study as discussed above.

Selective Adsorption of Lead, Copper, and Cadmium in Ion-Exchange Systems

As the coexisting ions not only compete for the vacant sites on the biosorbent but also for the occupied sites, it is likely that ion exchange would occur between metal ions in the liquid phase and in the solid (adsorbed) phase. Experiments were thus designed to observe the phenomena of ion exchange by the addition of metal B into the biomass that was already saturated with metal A. The behavior of ion exchange between metals A and B was then monitored as a function of the added metal B concentrations. The experimental results were analyzed quantitatively by the relative total adsorption capacity $Q_{A,B}$ and the replacement efficiency $R_{A,B}$. The parameter $Q_{A,B}$ represents the ratio of combined adsorption capacity of metal A and metal B versus the saturation capacity of metal B, and thus is a reflection of the change of total surface capacity relative to the saturation coverage of metal B during the ion-

TABLE 3
Average $R_{A,B}$ and $Q_{A,B}$ Values for Different Binary Combinations of Metals A and B in the Ion-Exchange Processes

Metal A (added)	Metal B (pre-adsorbed)	$R_{A,B}$ (%)	$Q_{A,B}$ (%)
Pb	Cu	32	106
Cu	Pb	27	160
Pb	Cd	55	150
Cd	Pb	10	105
Cu	Cd	45	170
Cd	Cu	26	103

exchange operation. The other parameter $R_{A,B}$ represents the percentage of the preadsorbed metal B replaced by ion exchange of added metal A ions. So, $R_{A,B}$ directly indicates the strength of ion exchange of metal A over metal B. It was a general trend that after an initial increase with increased metal A concentration, the values of $Q_{A,B}$ and $R_{A,B}$ were essentially invariant as metal A concentration was over 1000 μmol/L until the experiment was terminated at 3000 μmol/L. Therefore, the average $Q_{A,B}$ and $R_{A,B}$ values during that invariant range for different binary combinations of metal A and B are demonstrated in Table 3 to provide simplified quantitative views of the ion-exchange processes. Table 3 shows that $R_{Pb,Cu}$ and $R_{Cu,Pb}$ values were similar at 32% and 27%, respectively, suggesting that lead and copper ions exhibited comparable strength in replacing each other from the biomass. However, since $R_{Pb,Cd}$ and $R_{Cu,Cd}$ values were 2–5-fold greater than $R_{Cd,Cu}$ and $R_{Cd,Pb}$ (Table 3), it is clear that Pb and Cu both dominated Cd ions during the ion-exchange process. It is also observed from Table 3 that $Q_{Pb,Cu}$, $Q_{Cd,Pb}$, and $Q_{Cd,Cu}$ values were approximately equal to 100%, whereas $Q_{Cu,Pb}$, $Q_{Pb,Cd}$, and $Q_{Cu,Cd}$ values were way above 100%. A 100% $Q_{A,B}$ value means that after the addition of metal A onto the metal B-saturated biomass, the total capacity of the biomass for metals A and B together is equal to the previous saturation capacity of metal B. That is, the amount of metal A adsorbed is equal to the amount of metal B replaced. In contrast, when $Q_{A,B}$ values exceed 100% there may be a possibility of insertion of metal A on the surface sites beyond the saturation coverage of metal B. Therefore, the results tend to show that there was no vacant site available for Pb and Cd on the surface saturated by copper, so adsorption of Pb and Cd on that surface was mainly due to ion exchange, which was also the major driving force triggering Cd adsorption on Pb-covered surface. It can also be justified from the $Q_{Cu,Pb}$ (160%) and $Q_{Cu,Cd}$ (170%) values that

a considerable part of Cu adsorption on Pb- and Cd-covered biomass was probably due to the insertion onto the surface sites which are not the inherent adsorption sites for Pb and Cd. Likewise, the insertion of Pb on vacant sites of the Cd-saturated surface may also take place, resulting in a $Q_{Pb,Cd}$ value of 150%. This seems to suggest that the biomass had more adsorption sites for Cu than for Pb and Cd, and that adsorption sites for Pb and Cd on the biomass were included in those for Cu, which is also in accord with the proposed surface coverage distribution model presented in Fig. 5. Moreover, since the saturation capacity of the biomass for Cu was about 15% higher than that for Pb (Table 1), it is not surprising to observe that $Q_{Cu,Pb}$ values exceeded 100%. The $Q_{Cu,Cd}$ and $Q_{Pb,Cd}$ values were as high as 170 and 150% respectively, which may be correlated to the ratio of the single-metal saturation capacity of the biomass (Table 1) between Cu and Cd (193%) and that between Pb and Cd (159%).

Models for Selective Biosorption Equilibria in Multimetal Systems

Model 1

This model is a multicomponent version of the traditional Langmuir isotherm. The major assumption of Model 1 is that the surface sites are uniform, so that the adsorbates (Pb, Cu, and Cd) compete for the same surface sites. The final expression of Model 1 can be described as follows (17):

$$q_i = \frac{q_{max} K_i Ce_i}{1 + K_i Ce_i + K_j Ce_j + K_k Ce_k} \tag{1}$$

where q_i: fraction of surface sites covered by adsorbate i (μmol i/g dry cell)

q_{max}: maximum capacity of the biosorbent for adsorbate (μmol i/g dry cell)

Ce_i: concentration of adsorbate i in liquid phase (μmol/L)

$$K_i = \frac{k_{a,i}}{k_{d,i}} = \frac{\text{adsorption rate constant of adsorbate } i \text{ } (h^{-1})}{\text{desorption rate constant of adsorbate } i \text{ (μmol } i\text{/h/L)}}$$

It should be noted that in this model the maximal capacity q_{max} is universal so that all three metals obey the fundamental hypothesis of the Langmuir model. To examine the validity of Model 1 for multicomponent adsorption systems, the experimental data shown in Figs. 1–4 were simulated numerically according to Eq. (1). Two parameters associated with Model 1, K_i and q_{max}, were estimated by utilizing MATLAB version 4.0. The optimal parameters estimated for Model 1 are listed in Table 4.

TABLE 4
Kinetic Parameters of Single and Multicomponent Adsorption Isotherms Estimated from Model 1

i (adsorbate)	q_{max} (μmol/g)	K_i (L/μmol)
Pb	520	$K_{Pb} = 0.0903$
Cu	632	$K_{Cu} = 0.0423$
Cd	327	$K_{Cd} = 0.0242$
Cu–Pb	630	$K_{Cu} = 0.0154$
		$K_{Pb} = 0.0114$
Cu–Cd	500	$K_{Cu} = 0.0115$
		$K_{Cd} = 0.00170$
Pb–Cd	510	$K_{Pb} = 0.0274$
		$K_{Cd} = 0.00180$
Pb–Cu–Cd	610	$K_{Pb} = 0.0213$
		$K_{Cu} = 0.0122$
		$K_{Cd} = 0.00133$

Model 2

For the model proposed in Fig. 5, the biomass of *P. aeruginosa* PU21 contained different maximal capacities for Pb, Cu, and Cd during their coexistence. This tends to suggest that the surface sites of the biosorbent were somehow nonhomogeneous, and some of the sites may be specific to certain adsorbates. The phenomenon is apparently inconsistent with the assumption of the conventional Langmuir model which is the basis for the derivation of Model 1. In order to describe the experimental results more correctly, the Langmuir model was modified by assuming different maximal adsorption capacities (q_{max}) for the adsorbates Pb, Cu, and Cd. Thus, as equilibrium is reached, the counterbalance of adsorption and desorption rates gives:

$$k'_{a,Cu}C_{e,Cu}(q_{max,Cu} - q_{Cu} - q_{Pb} - q_{Cd}) = k'_{d,Cu}q_{Cu} \quad (2)$$

$$k'_{a,Pb}C_{e,Pb}(q_{max,Pb} - p_{Cu,Pb}q_{Cu} - q_{Pb} - p_{Cd,Pb}q_{Cd}) = k'_{d,Pb}q_{Pb} \quad (3)$$

$$k'_{a,Cd}C_{e,Cd}(q_{max,Cd} - p_{Cu,Cd}q_{Cu} - p_{Pb,Cd}q_{Pb} - q_{Cd}) = k'_{d,Cd}q_{Cd} \quad (4)$$

where $q_{max,i}$ represents the maximal adsorption capacity of adsorbate i, $k'_{a,i}$ (g dry cell/μmol i/h) and $k'_{d,i}$ (g dry cell/h/L) are rate constants for adsorption and desorption of adsorbate i; and the parameter $p_{i,j}$ represents the probability that metal i adsorbs on the binding sites for metal j. Thus,

$$p_{i,j} = \frac{\text{common adsorption sites for metal } i \text{ and } j \text{ on the biosorbent}}{\text{total adsorption sites for metal } i \text{ on the biosorbent}}$$

According to the proposed adsorption-site distribution for Cu, Pb, and Cd shown in Fig. 5, we can calculate the values of $p_{Cu,Pb}$, $p_{Cd,Pb}$, $p_{Cu,Cd}$, and $p_{Pb,Cd}$ as 0.823, 0.847, 0.517, and 0.533, respectively.

By rearranging Eqs. (2), (3), and (4) individually, we are able to derive the expressions for q_{Cu}, q_{Pb}, and q_{Cd} as follows:

$$q_{Cu} = \frac{K'_{Cu}Ce_{Cu}(q_{max,Cu} - q_{Pb} - q_{Cd})}{1 + K'_{Cu}Ce_{Cu}} \tag{5}$$

$$q_{Pb} = \frac{K'_{Pb}Ce_{Pb}(q_{max,Pb} - p_{Cu,Pb}q_{Cu} - p_{Cd,Pb}q_{Cd})}{1 + K'_{Pb}Ce_{Pb}} \tag{6}$$

$$q_{Cd} = \frac{K'_{Cd}Ce_{Cd}(q_{max,Cd} - p_{Cu,Cd}q_{Cu} - p_{Pb,Cd}q_{Pb})}{1 + K'_{Cd}Ce_{Cd}} \tag{7}$$

where K'_i (Langmuir constant) $= k'_{a,i}/k'_{d,i}$.

For given Ce_{Cu}, Ce_{Pb}, and Ce_{Cd} values, the corresponding q_{Cu}, q_{Pb}, and q_{Cd} values can be obtained by solving Eqs. (5), (6) and (7) simultaneously. Model 2 was used to describe the isotherms obtained from two-metal and three-metal adsorption, as illustrated in Figs. 1–4, and the corresponding optimal parameters are presented in Table 5.

Model 3

The major idea of this model originated from comparing the results of adsorption isotherms between single-metal and multimetal systems (Figs.

TABLE 5
Kinetic Parameters of Multicomponent Adsorption Isotherms Estimated from Model 2

i (adsorbate)	$q_{max,i}$	K'_i
Cu–Pb	$q_{max,Cu}$ = 634	K'_{Cu} = 0.00237
	$q_{max,Pb}$ = 521	K'_{Pb} = 0.0462
Cu–Cd	$q_{max,Cu}$ = 529	K'_{Cu} = 0.0111
	$q_{max,Cd}$ = 280	K'_{Cd} = 0.00652
Pb–Cd	$q_{max,Pb}$ = 520	K'_{Pb} = 0.0747
	$q_{max,Cd}$ = 320	K'_{Cd} = 0.00463
Cu–Pb–Cd	$q_{max,Cu}$ = 668	K'_{Cu} = 0.00492
	$q_{max,Pb}$ = 601	K'_{Pb} = 0.0122
	$q_{max,Cd}$ = 339	K'_{Cd} = 0.00124

1–3). It was observed that the adsorption equilibrium in single-metal systems was easily described by the conventional Langmuir-type isotherm, whereas the adsorption isotherms in multimetal systems deviated considerably from the single-metal isotherms due to the effect of the coexisting metals. Model 3 utilized the single-component Langmuir model as the starting structure, which was then combined with a logistic term to compensate for the deviation between single- and multicomponent isotherms. Therefore, the adsorption isotherm for a multicomponent system becomes

$$q_i = \frac{q_{\max,i} K_i Ce_i}{1 + K_i Ce_i} [1 - F_i(C)]_i \tag{8}$$

where $F_i(C)$ represents the fractional deviation of the multicomponent adsorption isotherm from the single-component Langmuir isotherm for adsorbate i. Note that the term $[1 - F_i(C)]_i$ is assumed to be specific for each q_i. The $F_i(C)$ was expressed as a logistic form as

$$F_i(C) = \frac{\sum_{\substack{j=1 \\ j \neq i}}^{N} Ki_j Ci_j}{\sum_{j=1}^{N} Ki_j Ci_j} \tag{9}$$

where Ci_j represents the initial concentration of adsorbate j, and Ki_j is a modification coefficient for adsorbate j.

According to Eqs. (8) and (9), the ternary form of Model 3 can be expressed as

$$q_{Pb} = \frac{q_{\max,Pb} K_{Pb} Ce_{Pb}}{1 + K_{Pb} Ce_{Pb}} \left[1 - \frac{Ki_{Cu} Ci_{Cu} + Ki_{Cd} Ci_{Cd}}{Ki_{Pb} Ci_{Pb} + Ki_{Cu} Ci_{Cu} + Ki_{Cd} Ci_{Cd}} \right]_{Pb} \tag{10}$$

$$q_{Cu} = \frac{q_{\max,Cu} K_{Cu} Ce_{Cu}}{1 + K_{Cu} Ce_{Cu}} \left[1 - \frac{Ki_{Pb} Ci_{Pb} + Ki_{Cd} Ci_{Cd}}{Ki_{Pb} Ci_{Pb} + Ki_{Cu} Ci_{Cu} + Ki_{Cd} Ci_{Cd}} \right]_{Cu} \tag{11}$$

$$q_{Cd} = \frac{q_{\max,Cd} K_{Cd} Ce_{Cd}}{1 + K_{Cd} Ce_{Cd}} \left[1 - \frac{Ki_{Pb} Ci_{Pb} + Ki_{Cu} Ci_{Cu}}{Ki_{Pb} Ci_{Pb} + Ki_{Cu} Ci_{Cu} + Ki_{Cd} Ci_{Cd}} \right]_{Cd} \tag{12}$$

It is preferable to describe Eqs. (10) to (12) in terms of initial concentrations of the adsorbates (Ci_i), so the equilibrium concentration Ce_i in the equations was replaced by $(Ci_i - q_i \times W_{cell})$, where W_{cell} is the total cell dry weight

TABLE 6
Kinetic Parameters of Two-Component Adsorption Isotherms Estimated from Model 3

i (adsorbate)	$q_{max,i}$	K_i	$K_{i_{Pb}}$	$K_{i_{Cu}}$	$K_{i_{Cd}}$
Pb	520	0.0904	0.699	0.400	0.0806
Cu	632	0.0417	0.374	0.281	0.120
Cd	327	0.0245	0.404	0.607	0.0792

in the adsorption mixture of interest. The parameters $q_{max,i}$, and K_i in Eqs. (10)–(12) were obtained from the single-metal adsorption isotherms, while Ki_j values were estimated from numerical simulations of two-metal adsorption data. The optimal parameters are presented in Table 6. It should be noted that there were three sets of Ki_{Pb}, Ki_{Cu}, and Ki_{Cd} values associated with q_{Pb}, q_{Cu}, and q_{Cd}, respectively, since Eqs. (10)–(12) were simulated independently to determine each set of Ki_j. In order to avoid redundant parameter estimation procedures and to reduce the number of parameters required, prediction of three-component adsorption results by Model 3 was accomplished by using the parameters Ki_j estimated from binary systems. Comparison of the simulated results with the corresponding experimental data is shown in Figs. 1–4.

Justification of the Proposed Models

The variance between experimental data and the model prediction (Figs. 1–4) is summarized in Table 7, which shows that the prediction by Model 3 was most accurate for binary adsorption while Model 2 gave the best description for ternary adsorption results. Model 1 had the largest variance in both cases. As Model 2 described the experimental results more precisely than Model 1, the modification over traditional Langmuir kinetics turned out to improve the feasibility of the model. Generally speaking, all three models had better description (lower variance) for the data from Cu–Cd and Pb–Cu systems. However, the model had larger deviations on interpreting binary adsorption of Pb and Cd, probably because the inhibition effect of Pb on the adsorption of Cd was most significant in all binary systems. In contrast to the prediction for binary systems, the models generally showed better fits to the data from ternary systems. One of the reason for this phenomena may be ascribed to a higher degree of freedom for the ternary systems.

The Langmuir constants (K_i, K_i') associated with Models 1 and 2 are characteristic of the affinity of the metal ions to the biomass. Tables 4 and 5 indicate that the magnitude of those constants essentially followed a trend of Pb >

TABLE 7
The Variance between Experimental Data and Model Prediction

System	Mean square of residuals[a]	Number of experimental data
Pb–Cu:		
Model 1	6487.3	8
Model 2	841.6	8
Model 3	598.2	8
Pb–Cd:		
Model 1	3226.9	8
Model 2	2940.2	8
Model 3	1129.7	8
Cu–Cd:		
Model 1	1591.6	8
Model 2	294.0	8
Model 3	145.0	8
Cu–Pb–Cd:		
Model 1	567.0	27
Model 2	183.9	27
Model 3[b]	556.5	27

[a] Mean square of residuals

$$= \frac{\Sigma(\text{model prediction} - \text{experimental data})^2}{\text{number of experimental data}}.$$

[b] Using the parameters determined from binary systems to predict the adsorption equilibria from three-metal adsorption systems.

Cu > Cd, except for the Cu–Pb system in Model 1. These results further confirm that adsorption of Pb was most favored by the biomass, but which had the least preference for Cd. Similar conclusions can be drawn from Model 3 by comparing the value of Ki_j. From the definition of $F_i(C)$ indicated in Eqs. (8) and (9), the parameter Ki_j is considered as a weighting factor of adsorbate j for its strength to cause the deviation of the adsorption of coadsorbates from their single-metal adsorption isotherms. With this interpretation, metals with higher Ki_j values would exhibit stronger inhibition to the adsorption of other coexisting metals, and thus had higher adsorption dominance (or preference) for the adsorption sites. Table 6 shows that in all cases Ki_{Cd} was the lowest among the three modification coefficients, and the Ki_{Pb} was greater than Ki_{Cu} excluding the case of Cd adsorption in the presence of Pb and Cu (Eq. 12). Therefore, the trend of Ki_j values from Model 3 also supports our findings on the order of metal affinity to the biomass.

ACKNOWLEDGMENTS

We gratefully acknowledge financial support from National Science Council of the Republic of China under Grants NSC-83-0402-E-035-002 and NSC-84-2214-E-035-004.

REFERENCES

1. C. C. Ruchloft, *Sewage Works J.*, *21*, 877 (1949).
2. M. Tsezos, *Can. Metall. Q.*, *24*, 141 (1985).
3. B. Volesky and Z. R. Holan, *Biotechnol. Prog.*, *11*, 235 (1995).
4. B. Volesky, *FEMS Microbiol. Rev.*, *14*, 291 (1994).
5. P. K. Wong, K. C. Lam, and C. M. So, *Appl. Microbiol. Biotechnol.*, *39*, 127 (1993).
6. B. Volesky and I. Prasetyo, *Biotechnol. Bioeng.*, *43*, 1010 (1994).
7. Y. Andres, H. J. MacCordick, and J. C. Hubert, *Appl. Microbiol. Biotechnol.*, *44*, 271 (1995).
8. J. S. Chang and J. Hong, *Biotechnol. Bioengr.*, *44*, 999 (1994).
9. J. S. Chang, R. Law, and C. C. Chang, *Water Res.*, *31*, 1651 (1997).
10. G. A. Jacoby, in *The Bacteria, Vol X* (I. C. Gunsalus, J. R. Sokatch, and L. N. Ornston, Eds.), Academic Press, Orlando, FL, 1986, p. 497.
11. P. W. Atkins, *Physical Chemistry*, Oxford University Press, New York, NY, 1990, p. 884.
12. A. Nakajima and T. Sakaguchi, *Appl. Microbiol. Biotechnol.*, *38*, 574 (1993).
13. R. P. deCarvalho, K. H. Chong, and B. Velosky, *Biotechnol. Prog.*, *11*, 39 (1995).
14. B. Mattuschka and G. Straube, *J. Chem. Tech. Biotechnol.*, *58*, 57 (1993).
15. L. Pighi, T. Pumpel, and F. Schinner, *Biotechnol. Lett.*, *11*, 275 (1989).
16. G. M. Bodner and H. L. Pardue, *Chemistry: An Experimental Science*, Wiley, New York, NY, 1989, p. A-6.
17. R. T. Yang, *Gas Separation by Adsorption Processes*, Butterworths, Boston, MA, 1987, p. 49.

Received by editor March 21, 1997
Revision received August 1997